Failure of the Hume-Rothery stabilization mechanism in the Ag_5Li_8 gamma-brass studied by first-principles FLAPW electronic structure calculations

2008 J. Phys.: Condens. Matter 20 275228

(http://iopscience.iop.org/0953-8984/20/27/275228)

IOP PUBLISHING JOURNAL OF PHYSICS: CONDENSED MATTER

J. Phys.: Condens. Matter **20** (2008) 275228 (11pp) doi:10.1088/0953-8984/20/27/275228

Failure of the Hume-Rothery stabilization mechanism in the Ag_5Li_8 gamma-brass studied by first-principles FLAPW electronic structure calculations

U Mizutani[1], R Asahi[2], H Sato[3], T Noritake[2] and T Takeuchi[4]

[1] Toyota Physical and Chemical Research Institute, Nagakute, Aichi 480-1192, Japan
[2] Toyota Central R & D Laboratories, Incorporated, Nagakute, Aichi 480-1192, Japan
[3] Department of Physics, Aichi University of Education, Kariya-shi, Aichi 448-8542, Japan
[4] Ecopotia Science Institute, Nagoya University, Furo-cho, Chikusa-ku, Nagoya 464-8603, Japan

Received 15 February 2008, in final form 24 February 2008
Published 6 June 2008
Online at stacks.iop.org/JPhysCM/20/275228

Abstract

The first-principles FLAPW (full potential linearized augmented plane wave) electronic structure calculations were performed for the Ag_5Li_8 gamma-brass, which contains 52 atoms in a unit cell and has been known for many years as one of the most structurally complex alloy phases. The calculations were also made for its neighboring phase AgLi B2 compound. The main objective in the present work is to examine if the Ag_5Li_8 gamma-brass is stabilized at the particular electrons per atom ratio $e/a = 21/13$ in the same way as some other gamma-brasses like Cu_5Zn_8 and Cu_9Al_4, obeying the Hume-Rothery electron concentration rule. For this purpose, the e/a value for the Ag_5Li_8 gamma-brass as well as the AgLi B2 compound was first determined by means of the FLAPW-Fourier method we have developed. It proved that both the gamma-brass and the B2 compound possess an e/a value equal to unity instead of $21/13$. Moreover, we could demonstrate why the Hume-Rothery stabilization mechanism fails for the Ag_5Li_8 gamma-brass and proposed a new stability mechanism, in which the unique gamma-brass structure can effectively lower the band-structure energy by forming heavily populated bonding states near the bottom of the Ag-4d band.

(Some figures in this article are in colour only in the electronic version)

1. Introduction

Through intensive efforts by Hume-Rothery, Bradley, Westgren and their coworkers in the 1920s, a combination of noble metals Cu, Ag and Au with polyvalent elements like Zn, Cd, Al, etc, was found to crystallize into the so called beta- and gamma-brass structures at the particular electron per atom ratio e/a equal to $3/2$ and $21/13$, respectively [1–4]. The former refers to the body-centered cubic (bcc) or A2 compound at high temperatures but which often transforms into the ordered CsCl-type or B2 compound at low temperatures, whereas the latter contains 52 atoms in its cubic unit cell and has been regarded as a structurally complex compound. Mott and Jones [5] discussed the e/a-dependent stability of the gamma-brass in terms of the Fermi surface–Brillouin zone interaction in the framework of the free-electron model and attributed its stabilizing mechanism to simultaneous contacts of the free-electron Fermi sphere with a total of 36 Brillouin zone planes formed by the set of {330} and {411} lattice planes, inside of which 90 states per 52 atoms in a unit cell or 1.731 states per atom can be accommodated.

It is of critical importance to elucidate the e/a-dependent stabilization mechanism or alternatively the Hume-Rothery stabilization mechanism on the basis of the first-principles band calculations for realistic compounds, whose electronic structure is no longer describable in terms of the free-electron model. Asahi *et al* [6] performed the first-principles FLAPW (full potential linearized augmented plane wave) electronic structure calculations for Cu_5Zn_8 and Cu_9Al_4 gamma-brasses, the crystal structures of which were available

in the literature [7], and demonstrated why these complex electron compounds are stabilized at $e/a = 21/13$ in spite of the different solute concentrations involved. In both compounds, a deep pseudogap was found at the Fermi level in the density of states (DOS) curve. At the energy eigenvalues immediately above and below the pseudogap at the symmetry point N of the Brillouin zone, an extremely large Fourier component in the FLAPW wavefunction outside the muffin-tin sphere was found at $|\mathbf{G}|^2 = 18$ corresponding to the center of the {330} and {411} zones in both gamma-brasses, where $\mathbf{G}$ is the reciprocal lattice vector in units of $2\pi/a$ with the lattice constant a. The pseudogap at the Fermi level was confirmed to open up as a result of the formation of stationary waves due to the resonance of electrons with the set of {330} and {411} lattice planes. The FLAPW-Fourier method described above was powerful enough to verify the Hume-Rothery stabilization mechanism for both Cu_5Zn_8 and Cu_9Al_4 gamma-brasses, while taking the Cu- and Zn-3d states into account.

In the early 1930s, gamma-brasses were further discovered in other binary alloy systems, whose e/a values were less reliably assigned than those in noble metals alloyed with polyvalent elements, like Cu_5Zn_8 and Cu_9Al_4. Ekman [8] reported the formation of the gamma-brass phase in the TM–Zn and TM–Cd (TM = Co, Fe, Ni, Pd, Rh and Pt) alloy systems. He pointed out that the formation range in these gamma-brasses was centered at TM_5Zn_{21} or 19.2 at.% TM and concluded that transition metal atoms apparently contribute no electrons to the valence band, provided the electron concentration of 21/13 still serves as a key role in the stabilization of these gamma-brasses. The gamma-brass structure was found in other types of transition metal alloy systems. For example, Brandon *et al* identified the Al_8V_5 compound to possess the gamma-brass structure with the space group $I\bar{4}3m$ and speculated the electron concentration to be 76 electrons per 52-atom cell, i.e. $e/a = 1.46$, by assuming that each V atom absorbs one electron from those donated by Al in its hybridized bands having mainly d-character [9]. As is clear from the argument above, the presumption that all gamma-brasses including the transition metal-bearing ones must be stabilized at $e/a = 21/13$ has been made without any theoretical support and remained uncertain even up to now.

A new method to evaluate the e/a value for the transition metal element within the framework of the FLAPW-Fourier method was developed for TM_2Zn_{11} (TM = Fe, Co, Ni and Pd) [10] and Al_8V_5 gamma-brasses [11]. Among them, the pseudogap was confirmed to be present at the Fermi level in the DOS and the $e/a = 21/13$ resonance mechanism, i.e. the Hume-Rothery stabilization mechanism, to be valid only in Ni_2Zn_{11} and Pd_2Zn_{11}. In the case of the Al_8V_5 gamma-brass, for example, the DOS at the Fermi level is fully covered with the V-3d states. Here the V-3d states mediated resonance has been emphasized to play a key role in its stabilization [11]. In the determination of the e/a value for the TM element, the value of $2(\mathbf{k}_i + \mathbf{G})$ giving the largest Fourier component of the FLAPW wavefunction outside the muffin-tin sphere was extracted at a given energy eigenvalue, where $\mathbf{k}_i$ is selected at 200 points in the irreducible wedge corresponding to 1/48 of the reduced Brillouin zone of the body-centered cubic lattice. This determines a single-branch energy dispersion relation for electrons dominant outside the muffin-tin sphere. The value of $2(\mathbf{k}_i + \mathbf{G})$ at the Fermi level would correspond to the Fermi diameter for such itinerant electrons, from which the effective e/a value for the TM element was easily deduced. Small but positive e/a values of 0.15 and 0.07 were deduced for Ni and Pd in the Ni_2Zn_{11} and Pd_2Zn_{11} compounds, respectively [10]. The effective e/a value for the Al_8V_5 compound turned out to be $e/a = 1.94$, being different not only from the conventional value of $21/13 = 1.615$ but also that of 1.46 suggested by Brandon *et al* [9]. The effective e/a value for the V atom is deduced to be 0.23, since Zn is naturally assumed to be divalent. This demonstrated the existence of the gamma-brass, which must be excluded from those subjected to the Hume-Rothery electron concentration rule with $e/a = 21/13$.

In 1933, Perlitz [12] identified the Ag_3Li_{10} compound to crystallize into the same structure as that of the prototype gamma-brass Cu_5Zn_8 and to possess its lattice constant of 9.94 Å. This is seemingly at variance with the Hume-Rothery electron concentration rule for the gamma-brass, as long as valences of both Ag and Li are assumed to be unity. However, Hume-Rothery conjectured in the section dealing with 'Lithium and Its Abnormal Properties' of his textbook in 1962 [13] that the Ag_3Li_{10} gamma-brass would also be stabilized near 21/13, if lithium were divalent. No theoretical verification for his postulate on the e/a value of the Ag–Li gamma-brass has been so far attempted. To determine the e/a value and elucidate the stability mechanism of the Ag–Li gamma-brass by means of first-principles FLAPW band calculations, we need to have reliable crystal structure data. However, it remained less clear until recently because of the volatility and reactivity of lithium.

In 1972, Arnberg and Westman [14] reported for the first time the structure of the $Ag_{30.2}Li_{69.8}$ gamma-brass by analyzing measured powder x-ray diffraction data. They identified its structure as stacking the 26-atom cluster composed of 4, 4, 6 and 12 atoms at vertices of the inner tetrahedron (IT), outer tetrahedron (OT), octahedron (OH) and cubo-octahedron (CO), respectively, to form a body-centered cubic lattice with the space group $I\bar{4}3m$ (see figure 1). However, the reliability factor R_I was reduced to only about 10% because of the difficulty of its handling in air. More recently, Noritake *et al* [15] prepared the $Ag_{36}Li_{64}$ gamma-brass, the oxidation of which was minimized by conducting all operations in a glove box with flowing purified argon gas and reliably determined its crystal structure by analyzing the powder diffraction pattern taken with the use of a synchrotron radiation beam. They found that the Li atom enters exclusively into IT and CO sites, whereas the Ag atom into those on OT and OH sites in the 26-atom cluster but that small amounts of Li are mixed into OT and OH sites, resulting in chemical disorder.

In the present work, we performed the first-principles FLAPW band calculations with the assistance of the nearly-free-electron (NFE) and the LMTO–ASA (linear muffin-tin orbital–atomic sphere approximation) methods for the Ag_5Li_8 gamma-brass as well as the AgLi B2 compound by making full use of the experimentally determined crystal structures [15]. The e/a value for both phases was first determined by means

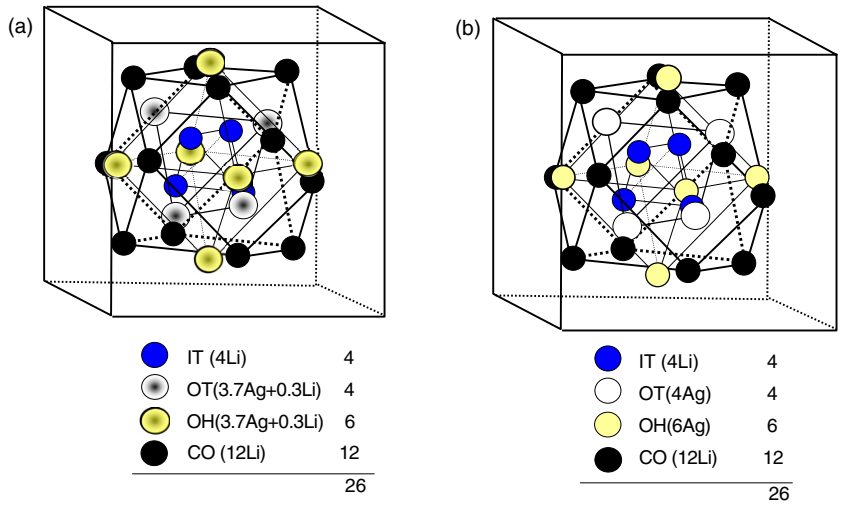

Figure 1. (a) Experimentally determined structure of Ag_5Li_8 gamma-brass [15] and (b) an ordered structure model employed in the present band calculations.

of the FLAPW-Fourier method. We demonstrated the failure of the Hume-Rothery stabilization mechanism for the Ag_5Li_8 gamma-brass and proposed a new mechanism responsible for stabilizing this particular phase.

2. Crystal structure

2.1. Ag_5Li_8 gamma-brass

As mentioned in the introduction, chemical disorder slightly exists in the experimentally determined crystal structure of the $Ag_{36}Li_{64}$ gamma-brass [15]. Its structure is reproduced in figure 1(a). Chemical disorder must be avoided in first-principles electronic structure calculations. An ordered structure is constructed simply by ignoring the small amount of Li atoms on OT and OH sites, where Ag atoms are otherwise occupied. This was made with a minimum sacrifice from the best-refined structure [15]. The ordered Ag_5Li_8 gamma-brass with the lattice constant of 9.9066 Å is adopted, as shown in figure 1(b). It may be noted that 61.5 at.% Li concentration in Ag_5Li_8 is slightly off from the limiting concentration of 63.5 at.% Li in the gamma-brass phase field in the equilibrium phase diagram [16].

2.2. AgLi B2 compound

Noritake *et al* also determined the lattice constant of the $Ag_{41.1}Li_{58.9}$ beta-phase alloy to be 3.1818 Å [15]. Note that the beta phase has a finite solid solution range [16]. The Li concentration in the sample above was off from that in the equiatomic AgLi B2 compound. The lattice constant for the B2 compound reported in the literature [17] is 3.168 Å, which is smaller than that of the Li-rich one. We chose the literature data [17] in the present work, since a decrease in the lattice constant is naturally expected from the difference in atomic radii of the constituent elements ($r_{Li} = 1.562$ Å and $r_{Ag} = 1.445$ Å).

3. Electronic structure calculations

3.1. First-principles FLAPW method

The details of the present FLAPW electronic structure calculations have been described elsewhere [18]. Briefly, the wavefunction is expressed as

$$\psi_i(\mathbf{r}, \mathbf{k}) = \sum_{\mathbf{G}} C^i_{\mathbf{k}+\mathbf{G}} \phi(\mathbf{r}, \mathbf{k}+\mathbf{G}), \tag{1}$$

where $\mathbf{k}$ is an arbitrary wavevector in the irreducible Brillouin zone, $\mathbf{G}$ is a reciprocal lattice vector and i is the band index. Here the basis functions are given as [18, 19]

$$\phi(\mathbf{r}, \mathbf{k}+\mathbf{G}) = \begin{cases} \Omega^{-1/2} e^{i(\mathbf{k}+\mathbf{G})\cdot\mathbf{r}} & r \in \text{interstitial} \\ \sum_{lm} [A^\alpha_{lm}(\mathbf{k}+\mathbf{G}) u_l(E^\alpha_l, r_\alpha) + B^\alpha_{lm}(\mathbf{k}+\mathbf{G}) \\ \quad \times \dot{u}_l(E^\alpha_l, r_\alpha)] Y_{lm}(\hat{r}_\alpha) & r \in \text{sphere} \end{cases} \tag{2}$$

where $u(E^\alpha_l, r_\alpha)$ and $\dot{u}_l(E^\alpha_l, r_\alpha)$ are solutions of the radial Schrödinger equation solved at a fixed energy E^α_l and their derivatives, respectively, $Y_{lm}(\hat{r}_\alpha)$ is a spherical harmonic and the coefficients $A^\alpha_{lm}(\mathbf{k}+\mathbf{G})$ and $B^\alpha_{lm}(\mathbf{k}+\mathbf{G})$ are determined by the requirement that the plane waves and their radial derivatives are continuous at the surface of the muffin-tin spheres. The number of plane waves was about 2900 in the present Ag_5Li_8 gamma-brass.

3.2. NFE model

A total ionic potential $V(\mathbf{r})$ in a crystal is generally expressed as the sum of individual ionic potentials $V_\alpha(\mathbf{r} - \mathbf{R}_i - \mathbf{r}_j)$:

$$V(\mathbf{r}) = \sum_{i,j} V_\alpha(\mathbf{r} - \mathbf{R}_i - \mathbf{r}_j), \tag{3}$$

where α specifies atomic species Ag or Li, $\mathbf{R}_i$ runs over unit cells in the lattice and $\mathbf{r}_j$ over atoms in a unit cell [20].

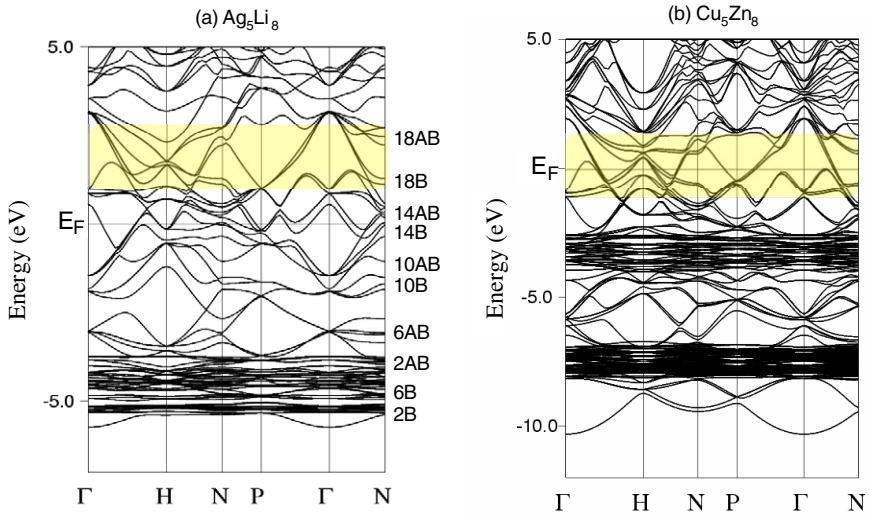

Figure 2. FLAPW-derived dispersion relations for (a) Ag_5Li_8 (present work) and (b) Cu_5Zn_8 gamma-brasses [6]. Yellow-colored regions refer to electronic states yielding the pseudogap in the respective DOSs. Numbers followed by AB (anti-bonding) and B (bonding) along the ordinate on the right-hand side in (a) refer to values of $|\mathbf{G}|^2$ or the sum of the Miller indices at the symmetry point N of the Brillouin zone. A yellow (or gray in black and white) zone in (a) and (b) is responsible for the formation of the pseudogap.

Equation (3) is expanded into a series with respect to the reciprocal lattice vector **G** in the system

$$V(\mathbf{r}) = \sum_{\mathbf{G}} V(|\mathbf{G}|)\exp(\mathrm{i}\mathbf{G}\cdot\mathbf{r}), \tag{4}$$

where the Fourier component of the potential within the local approximation [21] is called the form factor and is given by

$$V(|\mathbf{G}|) = \sum_{j}\left(\frac{1}{\Omega}\int V_\alpha(\mathbf{r})\mathrm{e}^{-\mathrm{i}\mathbf{G}\cdot\mathbf{r}}\mathrm{d}\mathbf{r}\right)\sum_{\mathbf{G}}\exp(-\mathrm{i}\mathbf{G}\cdot\mathbf{r}_i)$$
$$= \frac{1}{N}\sum_{j=1}^{N} V_\alpha(|\mathbf{G}|)\cos(\mathbf{G}\cdot\mathbf{r}_j), \tag{5}$$

where Ω is the volume of the system and the sum is taken over all atoms in a unit cell and the second line is reached when an inversion symmetry holds, as in the present case.

3.3. LMTO–ASA method

The LMTO–ASA electronic structure calculations were also made for the Ag_5Li_8 gamma-brass to extract information about orbital hybridizations (a) between Ag-4d and Ag-4d on atoms in OT and OH and (b) between Ag-4d on atoms in OT and OH, and Li-2sp states on atoms in IT and CO. The calculations were performed in the periodic zone scheme in combination with the local density functional theory, by using the crystal structure described in section 2. The potential parameters are self-consistently determined at 285 independent **k**-points in the irreducible wedge of the Brillouin zone for the Ag_5Li_8 gamma-brass [20].

4. Results

4.1. Electronic structure of the Ag_5Li_8 gamma-brass

Figure 2 shows the FLAPW-derived energy dispersion relations for (a) the present Ag_5Li_8 gamma-brass in comparison with (b) the prototype Cu_5Zn_8 gamma-brass reported earlier [6]. The congested bands in the binding energies centered at −4.5 eV in (a) and −7.5 and −3.0 eV in (b) are due to Ag-4d, Zn-3d and Cu-3d bands, respectively. The structure of dispersion relations marked by the yellow zone is very similar between (a) and (b) but the former is shifted to higher energies by about 2 eV relative to the latter with respect to the Fermi level. The corresponding FLAPW-derived DOSs for these two gamma-brasses are shown in figures 3(a) and (b). The sparse dispersions in the yellow zone in figure 2 obviously give rise to the pseudogap in the DOS at the energies centered at +2 eV in the Ag_5Li_8 and across the Fermi level in the Cu_5Zn_8.

As noted in section 1, the FLAPW-Fourier method for the Cu_5Zn_8 and Cu_9Al_4 gamma-brasses could identify the pseudogap at the Fermi level to originate from the resonance of itinerant electrons outside the muffin-tin sphere with the set of lattice planes {330} and {411} and deduce the effective e/a values to be close to 21/13 for both of them [6]. A resemblance of the energy dispersion relation in the yellow zone in the Ag_5Li_8 gamma-brass with that in the Cu_5Zn_8 gamma-brass strongly suggests the $|\mathbf{G}|^2 = 18$ resonance to be responsible for the formation of the pseudogap at about 2 eV above the Fermi level, as marked by an arrow in figure 3(a). More details will be discussed in section 5.1. Needless to say, its presence above the Fermi level can have nothing to do with stabilization of the Ag_5Li_8 gamma-brass phase.

4.2. Electronic structure of the AgLi B2 compound

The FLAPW-derived energy dispersion relations and the valence band DOS for the AgLi B2 compound are depicted in figures 4(a) and (b), respectively. The band centered at about-4.5 eV is obviously due to the Ag-4d states. The Fermi level is found to just touch the center of the {110} zone, which is

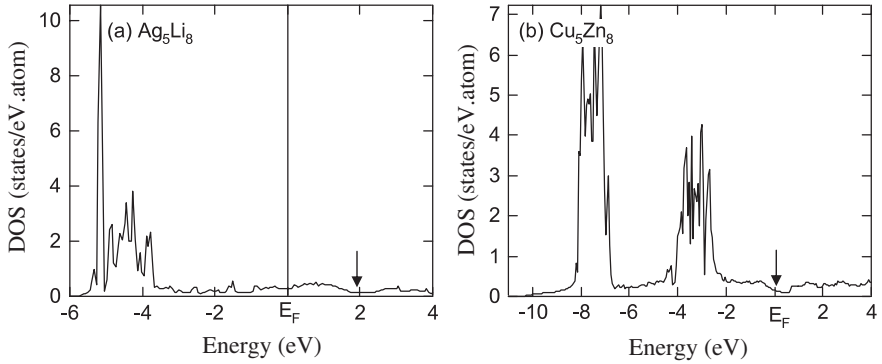

Figure 3. FLAPW-derived total DOSs for (a) Ag_5Li_8 (present work) and (b) Cu_5Zn_8 gamma-brasses [6]. An arrow in (a) indicates the pseudogap.

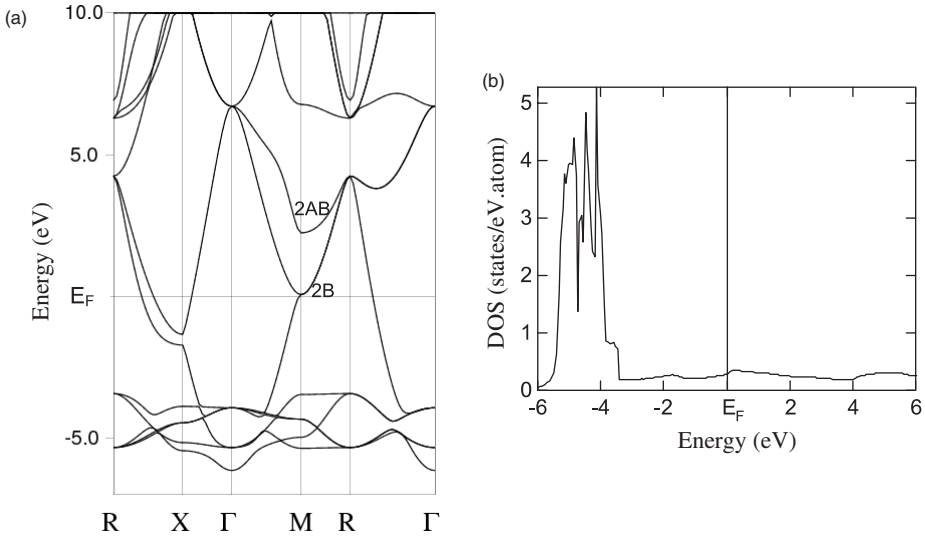

Figure 4. (a) FLAPW-derived energy dispersion relations for the AgLi B2 compound. Symbols '2AB' and '2B' refer to the anti-bonding and bonding states associated with $|\mathbf{G}|^2 = 2$, respectively, at the symmetry point M corresponding to the center of the {110} zone planes. (b) The valence band DOS derived from (a) for the AgLi B2 compound.

denoted as the symmetry point M in the CsCl-type structure. It is worth noting that a relatively large energy gap of about 2 eV across the {110} zone is taken as a manifestation of the deviation from the free-electron-like electronic structure due to the influence of d-states, as will be discussed later.

4.3. Determination of the effective e/a for the Ag_5Li_8 gamma-brass

The value of $2(\mathbf{k}_i + \mathbf{G})$ giving the largest Fourier component was deduced from the Fourier spectrum of the FLAPW wavefunction at a given energy eigenvalue, where $\mathbf{k}_i$ is selected at 200 points in the irreducible wedge (IBZ) corresponding to 1/48 of the reduced Brillouin zone [10, 11]. The quantity $k_G(E)$ is defined as

$$2k_G(E) \equiv 2\sum_{i=1}^{\mathrm{IBZ}} \omega_i |\mathbf{k}_i + \mathbf{G}|_E, \tag{6}$$

where i runs over the $\mathbf{k}_i$-points mentioned above, ω_ι is the weight associated with each $\mathbf{k}_i$-point and $|\mathbf{k}_i + \mathbf{G}|_E$ is evaluated at the energy E by linearly interpolating between energy eigenvalues. The IBZ over the symbol of summation indicates that the summation is taken over electronic states within the irreducible wedge of the Brillouin zone. The variance $\sigma^2(E)$ is defined as

$$\begin{aligned}\sigma^2(E) &= [2\{k_G(E) + \sigma_G(E)\}]^2 - \{2k_G(E)\}^2 \\ &= 8k_G(E)\sigma_G(E) + 4\sigma_G(E)^2,\end{aligned} \tag{7}$$

where the standard deviation $\sigma_G(E)$ is defined as

$$\sigma_G(E) \equiv \sqrt{\sum_{i=1}^{\mathrm{IBZ}} \omega_i (|\mathbf{k}_i + \mathbf{G}|_E - k_G(E))^2}. \tag{8}$$

Here the variance $\sigma^2(E)$ must be small enough to make $\{2k_G(E)\}^2$ well defined.

The resulting energy dependence of $\{2k_G(E)\}^2$ provides a single-branch dispersion relation in the extended zone scheme for electrons representing the FLAPW wavefunction outside the muffin-tin sphere. The value of e/a can be evaluated from the value of $\{2k_G(E)\}^2$ at the Fermi level, since it would

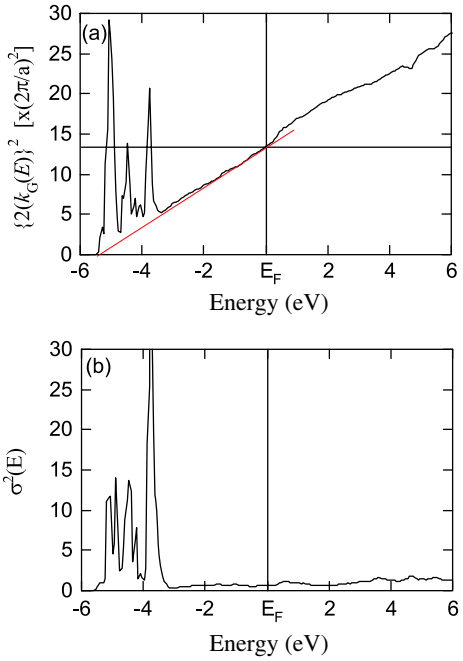

Figure 5. Energy dependence of (a) $\{2k_G(E)\}^2$ and (b) its variance $\sigma^2(E)$ calculated from equations (6)–(8) for the Ag_5Li_8 gamma-brass. The square of the Fermi diameter $(2k_F)^2$ is obtained by directly reading off the value of $\{2k_G(E)\}^2$ at the Fermi level. A straight line is drawn as a guide for the eyes.

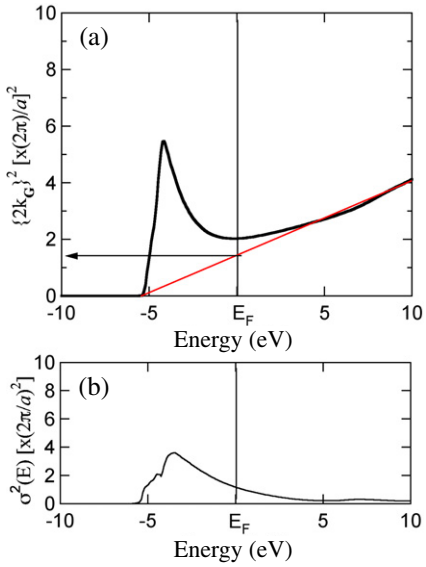

Figure 6. Energy dependence of (a) $\{2k_G(E)\}^2$ and (b) its variance $\sigma^2(E)$ calculated from equations (6)–(8) for the AgLi B2 compound. The square of the Fermi diameter $(2k_F)^2$ is obtained by reading off the value of $\{2k_G(E)\}^2$ at the Fermi level by extrapolating the data in energies above +4.5 eV to the Fermi level. The straight line passing through the origin is drawn as a guide for the eyes.

directly correspond to the square of the diameter of the Fermi sphere. Figure 5 shows the energy dependence of $\{2k_G(E)\}^2$ for the Ag_5Li_8 gamma-brass, along with that of the variance $\sigma^2(E)$. The value of $\sigma^2(E)$ over the range -5.5 to -3 eV is large, reflecting the presence of the Ag-4d states. Hence, values of $\{2k_G(E)\}^2$ in this energy range are meaningless. Instead, we can safely say that the value of $\{2k_G(E)\}^2$ is reliable over the range -3 up to about $+3$ eV, where $\sigma^2(E)$ is sufficiently small. Indeed, the data fall on a straight line, indicating that itinerant electrons outside the muffin-tin sphere behave almost in the free-electron fashion in this energy range.

The value of $\sigma^2(E)$ at the Fermi level, $\sigma^2(E_F)$, for various gamma-brasses studied so far is listed in table 1. They are classified into two groups (a) and (b), depending on whether the d-band exists below the Fermi level or dominates across the Fermi level. The Ag_5Li_8 gamma-brass characterized by a low value of $\sigma^2(E_F)$ certainly belongs to the former, together with Cu_5Zn_8, Cu_9Al_4 [6], Pd_2Zn_{11} and Ni_2Zn_{11} [10]. In group (a), we can directly read off the value of $\{2k_G(E)\}^2$ at the Fermi level. Instead, values of $\sigma^2(E_F)$ for Co_2Zn_{11}, Fe_2Zn_{11} [10] and Al_8V_5 [11] gamma-brasses in group (b) are high because of the presence of the d-band across the Fermi level. As emphasized earlier, the data below and above the d-band, where $\sigma^2(E)$ is sufficiently small, had to be extrapolated to the Fermi level to determine the square of the Fermi diameter $\{2k_G(E)\}^2$ in group (b).

The value of $\{2k_G(E)\}^2$ at the Fermi level for the Ag_5Li_8 gamma-brass turns out to be 13.4 from figure 5(a). This obviously represents the square of the Fermi diameter $(2k_F)^2$ for itinerant electrons outside the muffin-tin sphere. The

Table 1. $\sigma^2(E_F)$ of gamma-brasses.

Group (a)	$\sigma^2(E_F)$	Ref.	Group (b)	$\sigma^2(E_F)$	Ref.
Cu_5Zn_8	0.49	[6]	Co_2Zn_{11}	0.91	[10]
Cu_9Al_4	0.60	[6]	Fe_2Zn_{11}	1.44	[10]
Ni_2Zn_{11}	0.60	[10]	Al_8V_5	4.49	[11]
Pd_2Zn_{11}	0.56	[10]			
Ag_5Li_8	0.65	Present work			

effective e/a value for the Ag_5Li_8 gamma-brass is easily calculated to be 1.00 ± 0.02 by inserting $\{2k_F\}^2 = 13.4$ in units of $(2\pi/a)^2$ into the relation $e/a = \frac{8\pi k_F^3}{3N}$, where the number of atoms in the unit cell, N, is equal to 52. The valence of Li is confirmed to be unity, since that of Ag must be unity in the metallic state. We consider the present analysis to rule out clearly the Hume-Rothery postulate on divalence for Li [13].

4.4. Determination of the effective e/a for the AgLi B2 compound

Figure 6 shows the energy dependence of $\{2k_G(E)\}^2$ for the AgLi B2 compound, along with that of the variance $\sigma^2(E)$. In sharp contrast to the Ag_5Li_8 gamma-brass, both the departure of $\{2k_G(E)\}^2$ from a straight line and the magnitude of $\sigma^2(E)$ remain significant across the Fermi level, though the Ag-4d band is located far below the Fermi level (see figure 4(b)). The value of $\sigma^2(E_F)$ turned out to be 1.17, which is twice as large as that in the Ag_5Li_8 gamma-brass. The reason for this may be understood by analyzing the electronic states on the symmetry point M in figure 4(a). Obviously, the energy gap of about 2 eV in magnitude is opened up just above the Fermi level as a result of the interaction with the {110} zone planes with $|\mathbf{G}|^2 = 2$. The corresponding bonding

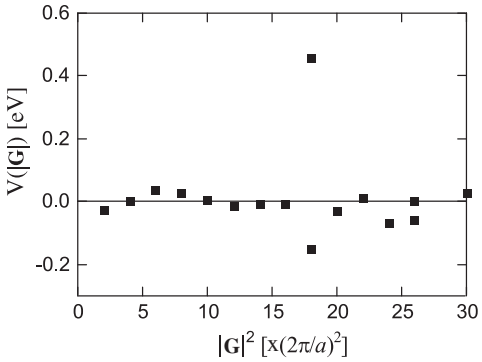

Figure 7. Form factor $V(|\mathbf{G}|)$ as a function of the square of the reciprocal lattice vector $|\mathbf{G}|^2$ for the Ag_5Li_8 gamma-brass.

and anti-bonding states are assigned as '2B' and '2AB', as marked in figure 4(a). This would naturally give rise to a heavily distorted Fermi surface for the AgLi B2 compound. Its anisotropy must be responsible for the possession of a large variance at the Fermi level. Instead, at the symmetry point N in the dispersion relation for the Ag_5Li_8 gamma-brass (see figure 2(a)), energy gaps associated with $|\mathbf{G}|^2 = 6$, 10 and 14 are relatively small. The ionic potentials around the Ag and Li atoms may well be screened by electrons in the energy range above -3 eV so that the more isotropic electronic structure is resumed near the Fermi level. In addition, the interaction of electronic states with the more spherical Brillouin zone, i.e. a total of 36 zone planes in the gamma-brass, would yield a more isotropic Fermi surface in the gamma-brass. These two effects would be combined to yield a well-suppressed variance over a wide energy range across the Fermi level. This must be one of the characteristic features in structurally complex electron compounds like the gamma-brass.

We could still roughly determine the value of $(2k_F)^2$ in the AgLi B2 compound by connecting almost linearly energy-dependent data above about $+4$ eV with data points very near the origin, where $\sigma^2(E)$ is sufficiently suppressed, as indicated in figure 6. The effective e/a value for the AgLi B2 compound was deduced to be 0.9 ± 0.1 from the resulting $(2k_F)^2 = 1.44$. In spite of a rather large uncertainty in determining the Fermi diameter, we took this as evidence for the possession of mono-valence for both Li and Ag in the AgLi B2 compound.

5. Discussion

5.1. Can zones satisfying the matching rule really form the pseudogap at the Fermi level?

We stressed in section 4.1 that the pseudogap formed at about 2 eV above the Fermi level in the Ag_5Li_8 gamma-brass can play no role in the stabilization. Thus, we need to seek for a stability mechanism, which must be different from that in the pseudogap-forming gamma-brasses like Cu_5Zn_8, Cu_9Al_4, Ni_2Zn_{11} and Pd_2Zn_{11}, where the Hume-Rothery electron concentration rule with $e/a = 21/13$ has been theoretically confirmed [6, 10]. Experimentalists have often discussed the stability of structurally complex compounds including quasicrystals by applying the $2k_F = |\mathbf{G}|$ matching

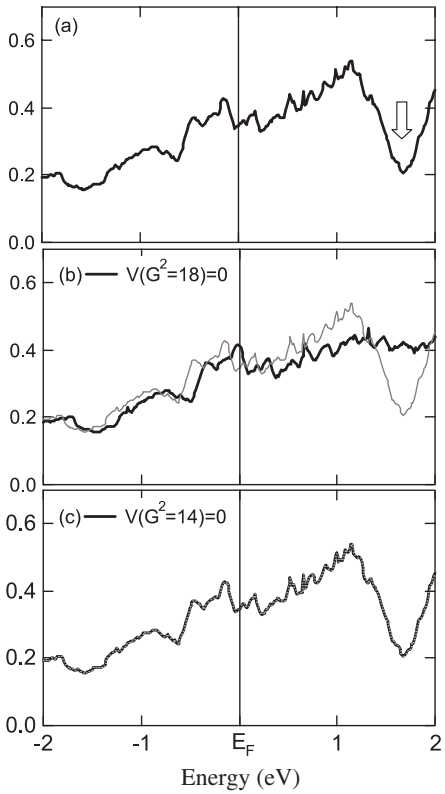

Figure 8. (a) NFE-derived DOS for the Ag_5Li_8 gamma-brass. A white arrow indicates the pseudogap. (b) DOS after zeroing the form factor $V(|\mathbf{G}|) = 18$ and (c) DOS after zeroing the form factor $V(|\mathbf{G}|) = 14$. The original DOS in (a) is reproduced as a gray curve in (b) and (c) as reference. But it is hardly visible in (c) because of its perfect superposition.

condition [22], which is deduced as a direct consequence from the Mott–Jones theory based on the free-electron model [5]. The application of the matching condition to the Ag_5Li_8 gamma-brass, for which $(2k_F)^2$ is theoretically proved to be 13.4, immediately specifies $|\mathbf{G}|^2 = 14$ as a set of lattice planes interacting with electrons at the Fermi level.

As has been discussed above, the Ag-4d band centered at about -4.5 eV may well be ignored in discussing electronic states near the Fermi level in the gamma-brass. The NFE model was employed while ignoring the Ag-4d states to study the effect of the resonance of itinerant electrons with different sets of lattice planes on the DOS. The form factor $V(|\mathbf{G}|)$ is shown in figure 7. It is extremely large only at $|\mathbf{G}|^2 = 18$ corresponding to the {330} and {411} zone planes for the Ag_5Li_8 gamma-brass.

The DOS calculated in the NFE model over the energy range -2 to $+2$ eV across the Fermi level is shown in figure 8(a). The pseudogap marked by a white arrow reproduces well that derived from the FLAPW method shown in figure 3(a). The effect of the deletion of the form factors $V(|\mathbf{G}|^2 = n)$ with $n = 18$ and 14 on the NFE-DOS is depicted in figures 8(b) and (c), respectively. The pseudogap at about $+2$ eV mentioned above is almost completely eliminated from the DOS calculated under the condition $V(|\mathbf{G}|^2 = 18) = 0$, confirming that it is definitely caused by the resonance of electrons with the set of lattice planes {330} and {411}. Instead,

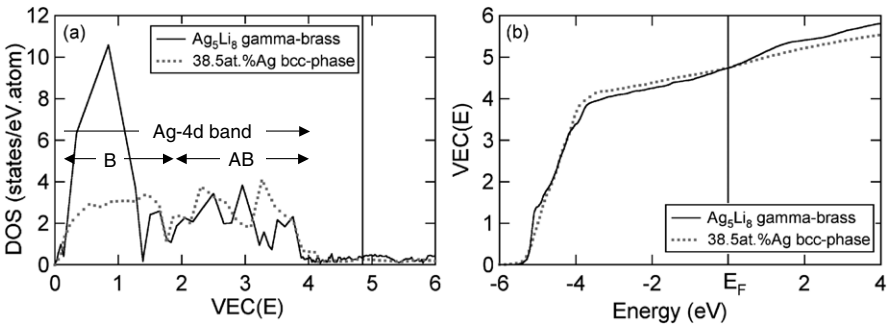

Figure 9. (a) The renormalized DOS as a function of $VEC(E)$ for the 38.5 at.% Ag bcc phase along with that for the Ag_5Li_8 gamma-brass calculated from figure 3(a). The vertical line represents the Fermi level, below which 4.85 electrons per atom are accommodated for both phases. (b) Energy dependence of $VEC(E)$ calculated from equation (11) for the Ag_5Li_8 gamma-brass and AgLi B2 compound. Symbols 'B' and 'AB' represent the bonding and anti-bonding states in the Ag-4d band, respectively.

the elimination of the form factor with $|\mathbf{G}|^2 = 14$ is found to hardly affect the DOS across the Fermi level. This is entirely consistent with the absence of a significant dip at the Fermi level in the FLAPW-DOS shown in figure 3(a).

All the arguments above led us to conclude that the $2k_F = |\mathbf{G}|$ condition with $|\mathbf{G}|^2 = 14$ does not play any critical role in the stabilization of the Ag_5Li_8 gamma-brass and that a mechanism other than the resonance of electrons with lattice planes has to be sought.

5.2. Phase stability of the Ag_5Li_8 gamma-brass relative to the AgLi B2 compound

The absence of a sizable pseudogap at the Fermi level in the Ag_5Li_8 gamma-brass makes studies of its stability mechanism more difficult. We must consider the stability of the Ag_5Li_8 gamma-brass relative to that of the AgLi B2 compound, more specifically, that of the bcc phase possessing the same amount of Ag as in the gamma-brass. According to density functional theory [23], the stability of a system at absolute zero is determined by the minimization of the total energy per atom, which is expressed as

$$U = \sum_i \varepsilon_i - \frac{1}{2}\int\int \frac{n(\mathbf{r})n(\mathbf{r}')}{|\mathbf{r}-\mathbf{r}'|}\,\mathrm{d}\mathbf{r}\,\mathrm{d}\mathbf{r}' + \int n(\mathbf{r})[\varepsilon_{\mathrm{XC}}(n(\mathbf{r})) - \mu_{\mathrm{XC}}(n(\mathbf{r}))]\,\mathrm{d}\mathbf{r}, \quad (9)$$

where the first term $\sum_i \varepsilon_i$ is called the one-electron band-structure energy and the second and third terms represent contributions from the electron–electron repulsion and the exchange–correlation effects, respectively. Here the energy ε_i is the solution of the effective one-electron Schrödinger equation of a system: $[-\frac{\hbar^2}{2m}\nabla^2 + v_{\mathrm{eff}}(\mathbf{r})]\psi_i(\mathbf{r}) = \varepsilon_i\psi_i(\mathbf{r})$. Since the quantitative evaluation of the second and third terms above is hard to make, we proceed with our discussion by assuming the phase stability to be exclusively determined by the band-structure energy of the individual phases:

$$U_{\mathrm{band}} = \int_{E_0}^{E_F} (\varepsilon - E_0)\cdot D(\varepsilon)\,\mathrm{d}\varepsilon, \quad (10)$$

where E_F, $D(\varepsilon)$ and E_0 are the Fermi level, the DOS and the energy of the bottom of the valence band of a given phase. This is essentially the approach taken by Jones [24] and Paxton *et al* [25]. The justification of the neglect of the electron–electron terms has been discussed within the framework of the LMTO–ASA method [26]. Below, the Fermi level in the upper limit of the integration in equation (10) is replaced by an arbitrary energy E to allow us to calculate the energy dependence of the band-structure energy $U_{\mathrm{band}}(E)$.

A caution should be noted upon comparing the band-structure energy of the Ag_5Li_8 gamma-brass with that of the AgLi B2 compound, since the Ag content involved, and hence the capacity of accommodating electrons in the Ag-4d bands in the respective DOSs, is different from each other. Indeed, total numbers of electrons per atom filled into the DOS for the Ag_5Li_8 gamma-brass and the AgLi B2 compound turn out to be 4.85 and 6.0, since Ag and Li atoms donate eleven and one electrons per atom, respectively. The number of electrons filled into the valence band is hereafter called the $VEC(E)$ or valence electron concentration to differentiate it from the effective e/a discussed in sections 4.3 and 4.4. In the case of the Ag–Li alloy system, the e/a is found to be unity, being independent of the Ag content, whereas the $VEC(E)$ increases with increasing Ag content. Rigorously speaking, the band-structure energy of the Ag_5Li_8 gamma-brass should be compared with that of the disordered bcc phase containing the same amount of Ag, i.e. 38.5 at.% Ag as in the gamma-brass. In the best we can do at the moment, we simply renormalized the DOS of the B2 compound by multiplying by a factor of 4.85/6.0 so as to reduce the value of the VEC to that of the gamma-brass.

In order to make the discussion more straightforward and transparent, we plotted in figure 9(a) the renormalized DOS, which is assumed to represent the DOS for the 38.5 at.% Ag bcc phase, as a function of $VEC(E)$ rather than the binding energy, along with the DOS of the Ag_5Li_8 gamma-brass reproduced from figure 3(a). Here the number of electrons per atom stored in the valence band up to energy E is calculated by integrating the DOS:

$$VEC(E) = \int_{E_0}^{E} D(\varepsilon)\,\mathrm{d}\varepsilon, \quad (11)$$

where E_0 is the energy of the bottom of the DOS, $D(E)$. Figure 9(b) confirms that the two curves representing the

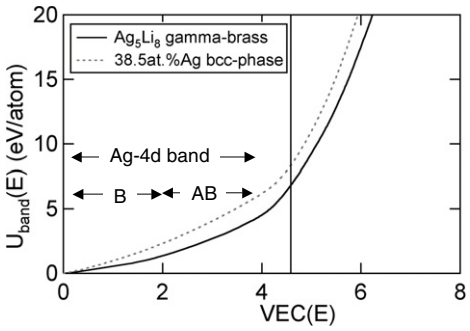

Figure 10. *VEC*(E) dependence of the band-structure energies per atom for both Ag_5Li_8 gamma-brass and the 38.5 at.% Ag bcc phase. Symbols 'B' and 'AB' represent the bonding and anti-bonding states in the Ag-4d band, respectively. The vertical line represents the Fermi level, below which 4.85 electrons per atom are accommodated for both phases.

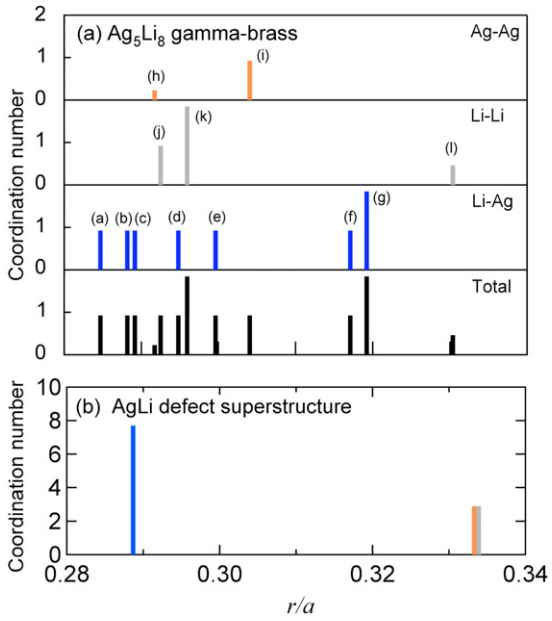

Figure 11. Radial distribution function (RDF) for (a) the Ag_5Li_8 gamma-brass and (b) the AgLi defect superstructure containing 52 atoms in its unit cell [15].

energy dependence of *VEC*(E) for both phases do meet at the Fermi level at the value of 4.85. The more interesting point in figure 9(b) is that *VEC*(E) jumps sharply by about 1.25 at $E = -5.15$ eV. This obviously arises from almost flat energy dispersions at the corresponding binding energies shown in figure 2(a). One can see from figure 9(a) that the Ag-4d bands for both phases are capable of accommodating approximately four electrons per atom and are roughly divided into bonding 'B' and anti-bonding 'AB' states over the ranges $0 \leqslant VEC(E) < 2.0$ and $2.0 < VEC(E) < 4.0$, respectively. A sharp rise in *VEC*(E) in figure 9(b) is certainly responsible for the growth of a large DOS in region B in figure 9(a). This unique feature is obviously absent in the counterpart B2 compound.

Now the band-structure energy per atom for the two phases is calculated by inserting the DOSs shown in figure 9(a) into equation (10). The resulting $U_{\rm band}(E)$ is plotted in figure 10 again as a function of *VEC*(E) for both phases. The value for the gamma-brass is found to be consistently lower over the whole *VEC*(E) range of interest than that for the 'bcc' phase having the renormalized DOS. More important is that the band-structure energy for the gamma-brass remains almost half that for the bcc phase at least up to $VEC(E) = 2.0$, corresponding to the bonding states marked as 'B' in the Ag-4d band. A significant suppression in the band-structure energy for the gamma-brass in region 'B' evidently stems from the fact that a large part of electrons in this region come from those participating in the *VEC*(E) jump mentioned above and that their contribution to the band-structure energy is small, since $(\varepsilon - E_0)$ in the integrand of equation (10) is small and almost constant. As is clear from figure 10, the gain in the band-structure energy created in region 'B' of the Ag-4d band for the gamma-brass relative to the bcc phase is not counterbalanced after *VEC*(E) passes the region 'AB' and even reaches the Fermi level corresponding to $VEC = 4.85$.

The difference in the band-structure energy $U_{\rm band}$ between the two phases amounts to 1.58 eV/atom or 150 kJ mol^{-1}. This is apparently too large, since a difference in the heat of formation between the two neighboring intermediate phases is generally of the order of several tens of kJ mol^{-1} [27]. We naturally expect the band-structure energy gained in region 'B' relative to a competing phase to be almost counterbalanced in region 'AB', resulting in only a small difference in the band-structure energy $U_{\rm band}$ between the two phases involved. Further work is certainly needed to elaborate the DOS for the 38.5 at.% Ag bcc phase by performing the first-principles band calculations coupled with the coherent potential approximation to treat a disordered alloy phase. Yet we believe the characteristic feature in region 'B' of the Ag-4d band to serve as a crucial clue for the stabilization of the Ag_5Li_8 gamma-brass.

5.3. Why unique bonding states 'B' are formed in the Ag-4d band of the Ag_5Li_8 gamma-brass?

Figure 11 shows the radial distribution function (RDF) for the Ag_5Li_8 gamma-brass calculated from the experimentally determined crystal structure [15], along with that of the defect superstructure AgLi, which is constructed by stacking three CsCl-type AgLi cells along the x, y and z directions and subsequently removing the center and corner atoms, resulting in 52 atoms in its unit cell. The RDF for the AgLi defect superstructure is identical to that for the AgLi B2 structure except for the slight reduction in the coordination numbers from eight nearest-neighbor pairs Ag–Li and six second-nearest-neighbor pairs Ag–Ag and Li–Li due to the removal of the two atoms. The gamma-brass structure can be obtained after slight reshuffling of atoms in the AgLi defect superstructure [2]. As discussed in the preceding section, however, the Ag concentration has to be decreased to 38.5 at.% to achieve the Ag_5Li_8 gamma-brass structure.

One can immediately recognize from figure 11 that the RDF spectra in the Ag_5Li_8 are widely spread over the r/a range from 0.285 to 0.305 and distances in the Ag–Li, Ag–Ag

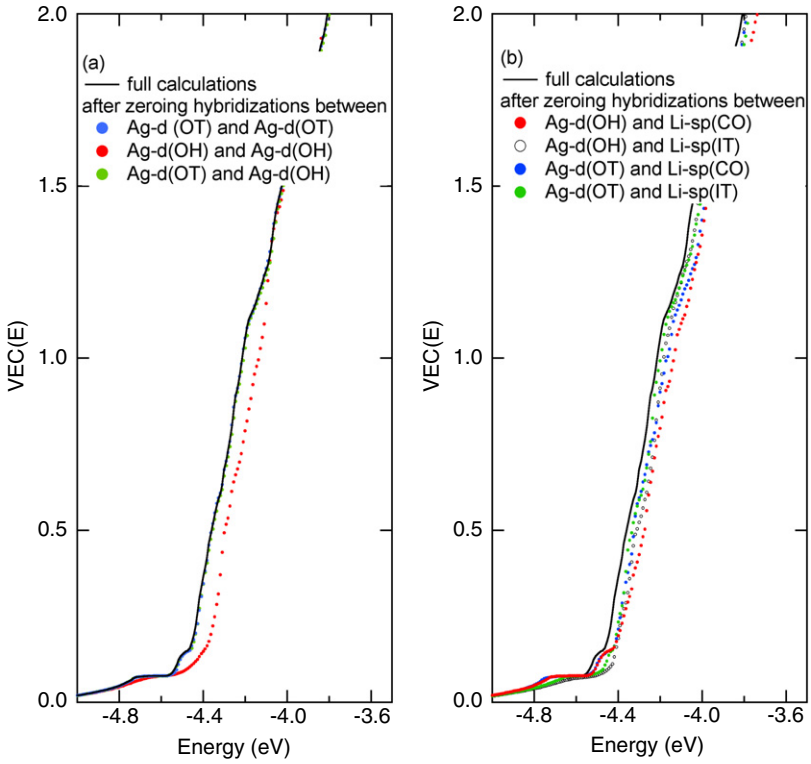

Figure 12. Energy dependence of $VEC(E)$ calculated from equation (11) in the framework of the LMTO–ASA method for the Ag_5Li_8 gamma-brass. The solid line refers to the data in the full calculations in both (a) and (b). A steep rise in the $VEC(E)$ over energies −4.2 to −4.5 eV corresponds to the $VEC(E)$ jump discussed in the text. The data in (a) obtained after the deletion of the Ag(OT)–Ag(OT) (blue dotted line) and Ag (OT)–Ag(OH) (green dotted line) pairs are almost fully superimposed onto those in the full calculations (solid line), indicating that these play no role in the formation of the flat bands in figure 2(a) or the $VEC(E)$ jump in figure 9(b). Instead, contributions from the Ag(OH)–Ag(OH) (red dotted line in (a)) and Ag(OH)–Li(CO) (red dotted line in (b)) pairs are the most significant.

and Li–Li pairs are substantially shortened. Thus, the gamma-brass structure is obviously sustained by a variety of bonding pairs in addition to an increase in the packing fraction of atoms relative to the B2 compound. The packing fractions of atoms in the gamma-brass structure and the AgLi B2 compound are 71 and 68%, respectively [28]. We believe that the appearance of Ag–Li and Ag–Ag bonding pairs in the gamma-brass shorter than those in the B2 structure must be linked with the formation of the unique bonding states 'B' in its Ag-4d band.

The LMTO–ASA method may be best suited for extracting the effect of orbital hybridizations between particular atomic pairs on the DOS or $VEC(E)$ calculated from equation (11) like that in figure 9(b). Figures 12(a) and (b) show the LMTO–ASA-derived $VEC(E)$–E curve for the Ag_5Li_8 gamma-brass in comparison with those after removing hybridization terms between Ag-4d and Ag-4d states on OT and OH and those between Ag-4d states on OT and OH, and Li-2sp states on IT and CO, respectively. First of all, a steep slope in $VEC(E)$ in the energy range over −4.2 and −4.5 eV is assigned as the FLAPW-derived $VEC(E)$ jump at $E = -5.15$ eV in figure 9(b) or region 'B' in figure 9(a)[5]. It can be seen from figure 12(a) that electronic states in region 'B' of the Ag-4d band are significantly contributed from the Ag(OH)–Ag(OH) pairs but not much from the Ag(OT)–Ag(OT) and Ag(OT)–Ag(OH) pairs. In the case of Ag–Li pairs, figure 12(b) identifies hybridizations due to Ag(OH)–Li(CO) pairs to affect most significantly electronic states in region 'B'. From the analysis above we can say that orbital hybridizations associated with Ag(OH)–Ag(OH) and Ag(OH)–Li(CO) pairs are critically important to produce the unique bonding states 'B' in the Ag-4d band.

All the arguments above led us to conclude that the splitting of the atomic pairs into twelve components (a)–(l) in the RDF spectrum causes the gamma-brass structure to be more stable over the bcc structure through redistribution of electrons, particularly the formation of the unique electronic structure near the bottom of the Ag-4d band.

6. Conclusions

The first-principles FLAPW electronic structure calculations with the assistance of the NFE and LMTO–ASA methods were performed for the Ag_5Li_8 gamma-brass and the AgLi B2 compound. The FLAPW-Fourier method revealed that the e/a values for both the Ag_5Li_8 gamma-brass and AgLi B2 compound are essentially equal to unity. This completely ruled out the Hume-Rothery postulate that the Ag_5Li_8 gamma-brass would obey the Hume-Rothery electron concentration rule with

[5] The LMTO–ASA-derived Ag-4d band happened to be centered at about −3.5 eV, being about 1 eV lower in binding energy than that derived from the FLAPW shown in figure 3(a). A $VEC(E)$ jump near the bottom of the Ag-4d band in figure 12 is visible but not as sharp as that shown in figure 9(b). But we consider these discrepancies to be unimportant in the present argument.

$e/a = 21/13$. We could also clearly demonstrate why the Hume-Rothery stabilization mechanism fails for the Ag_5Li_8 gamma-brass and alternatively proposed a new stabilization mechanism such that the gamma-brass structure yields unique bonding states in region 'B' of the Ag-4d band and contributes to effectively lowering its band-structure energy per atom relative to its bcc counterpart.

Acknowledgment

One of the authors (UM) acknowledges financial support of the Grant-in-Aid for Scientific Research (contract no. 1760583) from the Japan Society for the Promotion of Science.

References

[1] Hume-Rothery W 1926 *J. Inst. Met.* **35** 295–361
[2] Bradley A J and Thewlis J 1926 *Proc. R. Soc.* A **112** 678–92
[3] Westgren A and Phragmén G 1928 *Metallwirtschaft* **7** 700–703
[4] Westgren A and Phragmén G 1929 *Trans. Faraday Soc.* **25** 379–85
[5] Mott N F and Jones H 1936 *The Theory of the Properties of Metals and Alloys* (Oxford: Clarendon) pp 168–74
[6] Asahi R, Sato H, Takeuchi T and Mizutani U 2005 *Phys. Rev.* B **71** 165103
[7] Heidenstam O v, Johansson A and Westman S 1968 *Acta Chem. Scand.* **22** 653–61
[8] Ekman W 1931 *Z. Phys. Chem.* B **12** 57
[9] Brandon J K, Pearson W B, Riley P W, Chieh C and Stokhuyzen R 1977 *Acta Crystallogr.* B **33** 1088–95
[10] Asahi R, Sato H, Takeuchi T and Mizutani U 2005 *Phys. Rev.* B **72** 125102
[11] Mizutani U, Asahi R, Sato H and Takeuchi T 2006 *Phys. Rev.* B **74** 235119
[12] Perlitz H 1933 *Z. Kristallogr.* **86** 155
[13] Hume-Rothery W 1962 *Atomic Theory for Students of Metallurgy* (*Monograph and Report Series* vol 3) 4th edn (London: Institute of Metals) p 306
[14] Arnberg L and Westman S 1972 *Acta Chem. Scand.* **26** 1748–50
[15] Noritake T, Aoki M, Towata S, Takeuchi T and Mizutani U 2007 *Acta Crystallogr.* B **63** 726–34
[16] Okamoto H 2000 *Phase Diagrams for Binary Alloys* (Metals Park, OH: ASM International)
[17] Zintl E and Brauer G 1933 *Z. Phys. Chem.* B **20** 245–71
[18] Wimmer E, Krakauer H, Weinert M and Freeman A J 1981 *Phys. Rev.* B **24** 864
[19] Weinert M, Wimmer E and Freeman A J 1982 *Phys. Rev.* B **26** 4571
[20] Sato H, Takeuchi T and Mizutani U 2004 *Phys. Rev.* B **70** 024210
[21] Harrison W A 1979 *Electronic Structure and the Properties of Solids* (San Francisco, CA: Freeman) p 360
[22] Tsai A P 2005 *The Science of Complex Alloy Phases* ed T B Massalski and P E A Turchi (Warrendale, PA: The Minerals, Metals and Materials Society)
[23] Kohn W and Sham L J 1965 *Phys. Rev.* **140** A1133–8
[24] Jones H 1937 *Proc. Phys. Soc.* **49** 250–7
[25] Paxton A T, Methfessel M and Pettifor D G 1997 *Proc. R. Soc.* A **453** 1493–514
[26] Skriver H L 1985 *Phys. Rev.* B **31** 1909–23
[27] de Boer F R, Boom R, Mattens W C M, Miedema A R and Niessen A K 1988 *Cohesion in Metals* (Amsterdam: North-Holland)
[28] Brandon J K, Brizard R Y, Pearson W B and Tozer D J N 1977 *Acta Crystallogr.* B **33** 527–37